Discerning influences of orientational instability on anomalously roughened interfaces

Ning-Ning Pang[1] and Wen-Jer Tzeng[2]
[1]*Department of Physics, National Taiwan University, Taipei, Taiwan, Republic of China*
[2]*Department of Physics, Tamkang University, Tamsui, Taipei, Taiwan, Republic of China*
(Received 1 June 1999)

We measure the influence of the orientational instability on the local interfacial widths of two classes of super-rough growth models, one displaying single scaling and the other spatial multiscaling. For the former class, the anomalous dynamic scaling behavior is totally attributed to the orientational instability. Thus the local roughness relative to the average interfacial orientation in a local window of size l, $w_n(l,t)$, retrieves ordinary dynamic scaling behaviors. In contrast, for the latter class, the effect of the orientational instability is not the sole mechanism responsible for anomalously roughened interfaces; thus $w_n(l,t)$ still retains anomalous dynamic scaling behaviors.

PACS number(s): 05.40.−a, 47.55.Mh, 64.60.Ht, 68.35.Ct

The kinetic roughening phenomenon of growing interfaces [1] has brought about much interest not only for its important application in industry but also for the generic behavior widespread in nature's morphology. For example, the global interfacial widths $w(L,t)$ $(\equiv\overline{\langle [h(x,t)-\langle h(x,t)\rangle_L]^2\rangle_L}^{1/2})$, [with $h(x,t)$ denoting the interface height at position x and time t, $\langle\cdots\rangle_L$ the spatial average over the whole system of size L, and the overbar the statistical average], of the kinetically roughened surfaces have been known to obey the following dynamic scaling ansatz [2]: $w^2(L,t)=L^{2\chi}f(L/t^{1/z})$. For the correlation length $\xi\sim t^{1/z}\ll L$, $w(L,t)\sim t^{\beta}$ with $\beta=\chi/z$; for $\xi\sim t^{1/z}\gg L$, $w(L,t)[\equiv w_{sat}(L)]\sim L^{\chi}$, where $w_{sat}(L)$ is the saturated global width for systems of size L. χ and z are known as the *roughness exponent* and the *dynamic exponent*, respectively. Although the experimentally accessible quantities are actually the local interfacial width $w(l,t)$, measured over a local window of size l $(\ll L)$, and the height-difference correlation function $G(r,t)$ $(\equiv\overline{\langle [h(x_0,t)-h(x_0+r,t)]^2\rangle_L})$, people generally believe that the kinetically roughened interfaces are self-affine and, thus, the local interfacial width and the height-difference correlation function have the same scaling behavior as the global interfacial width.

Until recently, much attention was focused on the ''super-rough'' growth models, which are the growth models with the roughness exponent $\chi>1$. For various super-rough growth models, the behavior of the local interfacial width $w(l,t)$ and the height-difference correlation function $G(r,t)$, in the regime where the correlation length $\xi\sim t^{1/z}\ll L$, have been numerically observed to obey the following *anomalous dynamic scaling ansatz* [3–6] $w^2(l,t)=l^{2\chi}f_1(l/t^{1/z})$ and $G(r,t)=r^{2\chi}f_2(r/t^{1/z})$, where the scaling functions $f_{1,2}(y)\sim y^{-2\kappa}$ for $y\ll 1$ and $f_{1,2}(y)\sim y^{-2\chi}$ for $y\gg 1$. In contrast, for the usual dynamic scaling behavior, the scaling function goes to a constant quickly in the small y limit. Thus we see that systems with anomalous dynamic scaling behaviors consist of an extra independent exponent $\kappa(>0)$. Moreover, the nonsaturation of the scaling function $f(y)$ in the small y limit, the signature of anomalous dynamic scaling, gives rise to a substantial difference between global and local scaling behaviors. Quantitatively, we see that $w(l,t)\sim l^{\chi'}$ and $G(r,t)\sim r^{2\chi'}$, with $\chi'\equiv\chi-\kappa$, in the regime $r\leqslant l\ll t^{1/z}\ll L$ at a fixed time slice t. These anomalous dynamic scaling behaviors in the super-rough growth models are not only verified by various numerical works, but also observed in several experiments [7–10].

Qualitatively, the interfacial super-roughness is attributed to orientational instability toward the creation of large slopes. However, an extensive analysis of the influence of the orientational instability on the anomalously roughened interfaces is still lacking. Thus it is unclear whether orientational instability alone causes the nonsaturation of the local interfacial width in the regime $l\ll t^{1/z}\ll L$. This motivates us to quantitatively measure the influence of the orientational instability on local interfacial widths of various super-rough growth models. In order to clarify this issue, we first propose a new definition of the local interfacial width $w_n(l,t)$ as follows: $w_n^2(l,t)\equiv\overline{\langle\langle [h(x,t)-\tilde{h}(x,t)]^2\rangle_l\rangle_L}$, which is the roughness of the interface relative to the average interfacial orientation in a local window of size l. Here $h(x,t)$ denotes the interface heights, measured from the substrate, on a linear lattice $x=1,2,\ldots,L$, while $\tilde{h}(x,t)$ denotes the heights of a straight line obtained by a least squares fit to the interfacial configuration in a local window of size l at a given time t. Quantitatively, $\tilde{h}(x,t)=\langle h(x,t)\rangle_l+(x-\langle x\rangle_l)\,s(l,t)$, with the local orientation $s(l,t)=[12/(l^2-1)]\ \langle (x-\langle x\rangle_l)\,h(x,t)\rangle_l$, where $\langle\cdots\rangle_l$ denotes the spatial average calculated within a local window of size l. Subsequently, $w_n(l,t)$ is obtained by averaging over many local windows of the same size l along the interface, and then over the randomness. Consequently, the original local width $w(l,t)$ and the modified local width $w_n(l,t)$ are related as follows: $w^2(l,t)-w_n^2(l,t)=[(l^2-1)/12]\ \overline{\langle s^2(l,t)\rangle_L}$. Thus the measurement of $[w^2(l,t)-w_n^2(l,t)]^{1/2}$, which is proportional to the magnitude of the slope of the local interfacial configuration, extracts the information related to the effect of orientational instability.

Next we undertake extensive numerical studies on two major classes of super-rough growth models, one displaying single scaling behaviors and the other spatial multiscaling behaviors. We choose two distinct paradigmatic growth

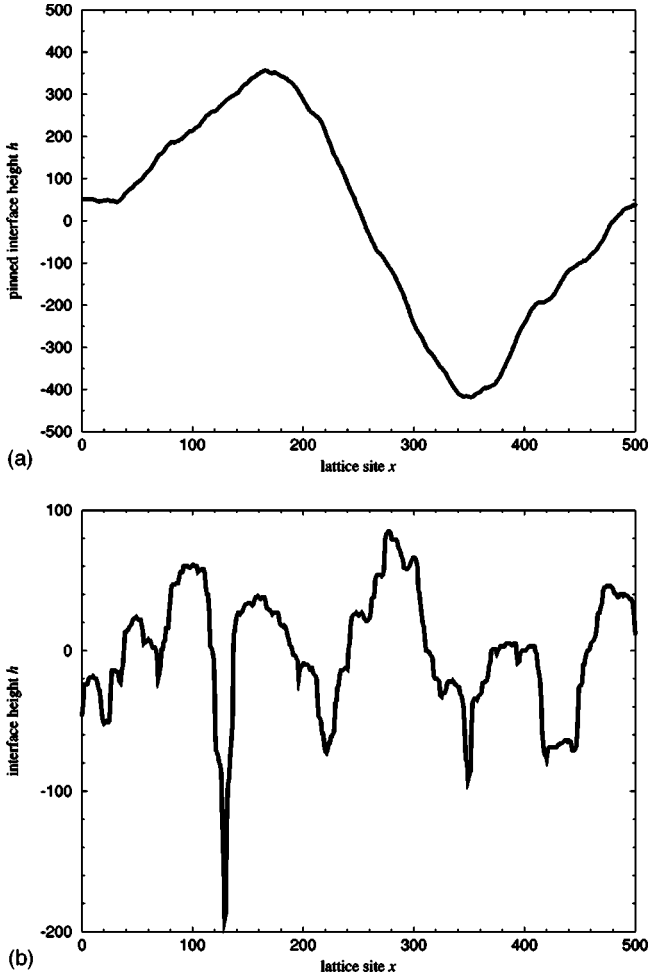

FIG. 1. The interfacial configurations $h(x,t)$ vs the lattice site x for (a) the Leschhorn model pinned at $p=p_c$ and (b) the DT model at time $t=65536$ ML. In both figures, the zero points of heights are set equal to their respective average heights.

models for simulation: the Leschhorn model [11] for the former class, and the Das Sarma-Tamborenea (DT) model [12] for the latter class. The Leschhorn model can be viewed as the realization of the Edwards-Wilkinson type equation with quenched disorder [13,14] in a discrete space-time lattice. It has been shown [6] that this model, at the depinning transition, displays the interfacial super-roughness and single scaling behaviors. In contrast, the DT model, originally proposed to describe the mobility-limited surface-diffusion-driven growth mechanism in molecular-beam-epitaxy growth processes, serves as a paradigm for the behavior of super-rough growth models with spatial multiscaling [4]. For comparison, we also simulate the Family model [15], which is a discrete realization of the original Edwards-Wilkinson equation [16] with annealed white noise and displays truly self-affine interfacial behaviors and ordinary dynamic scaling.

For all three growth models studied here, the interface is represented by a set of integers $h(x,t)$ on a linear lattice $x=1,2,\ldots,L$. No overhangs are allowed. Flat initial conditions, i.e., $h(x,t=0)\equiv 0$ for all x, and periodic boundary conditions, i.e., $h(L+1,t)\equiv h(1,t)$ and $h(0,t)\equiv h(L,t)$, are imposed. The growth rules of the Leschhorn model [11] are as follows. Each site on a square lattice is assigned a random noise $\eta(x,h)$, taking a value 1 with probability p or -1 with

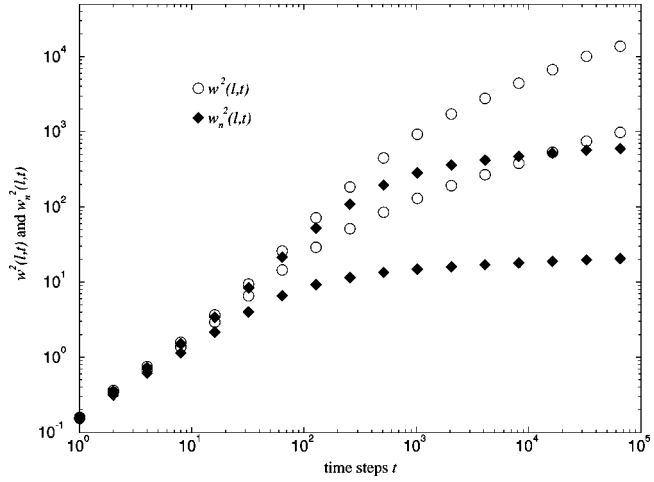

FIG. 2. The log-log plot of $w^2(l,t)$ (circle) and $w_n^2(l,t)$ (diamond) vs time t, for $l=32$ and 128 (from bottom to top), of the Leschhorn model at $p=p_c$.

probability $q=1-p$. The value v_x is defined as $v_x=h(x+1,t)+h(x-1,t)-2h(x,t)+g\,\eta(x,h)$. The parameters g and $q-p$ represent the relative strength of the random pinning force compared to the surface tension and the driving force, respectively. Then, at each time step t, the interface is updated simultaneously for all x: $h(x,t+1)=h(x,t)+1$ if $v_x>0$, and $h(x,t+1)=h(x,t)$ otherwise. For the other two models (the DT model and the Family model), random deposition occurs, and the time t is defined as the number of deposited layers. The relaxation rules of the DT model [12] are as follows: (1) Each site x on a linear lattice is associated with a coordination number n_x, which represents the number of occupied lateral nearest neighbors after an adatom deposited at some site y. (2) The adatom is allowed to relax to a nearest neighbor site only if $n_y=0$ and $n_{y'}>0$, with $y'=y-1$ or $y+1$. (3) If both n_{y-1} and n_{y+1} are larger than zero, one of the two sites is chosen at random. In contrast, the deposited adatom in the Family model [15] is allowed to relax to the site with the smallest resulting height among the deposited site and its nearest neighbor sites.

We first study the Leschhorn model. Fig. 1(a) shows a pinned interfacial configuration $h(x,t)$ vs a lattice site x, with the system size $L=512$ at the depinning transition $p=p_c\simeq 0.8004$ (for $g=1$) [11] for the Leschhorn model. Figure 1(a) shows the formation of a global groove with a horizontal size of the order of the system size L. The interfacial patterns for other super-rough growth models with single scaling behaviors [3,17] share a common characteristic: the formation of global grooves. We then numerically measure $w(l,t)$ and $w_n(l,t)$ in the Leschhorn model. The simulation is done with a system size $L=16384$ at $p=p_c$, and averaged over 100 realizations. Figure 2 shows a log-log plot of $w^2(l,t)$ (circle) and $w_n^2(l,t)$ (diamond) vs time t, for local window sizes $l=32$ and 128 (from bottom to top) of the Leschhorn model at $p=p_c$. The roughness exponent χ and the dynamic exponent z for the Leschhorn model are 1.23 ± 0.01 and 1.42 ± 0.02, respectively [6]. The saturation of $w_n(l,t)$ in the regime $l\ll t^{1/z}$ gives strong evidence that the anomalous time dependence of the original local width $w(l,t)$ in the long time regime can be solely attributed to the orientational instability, which allows large interfacial

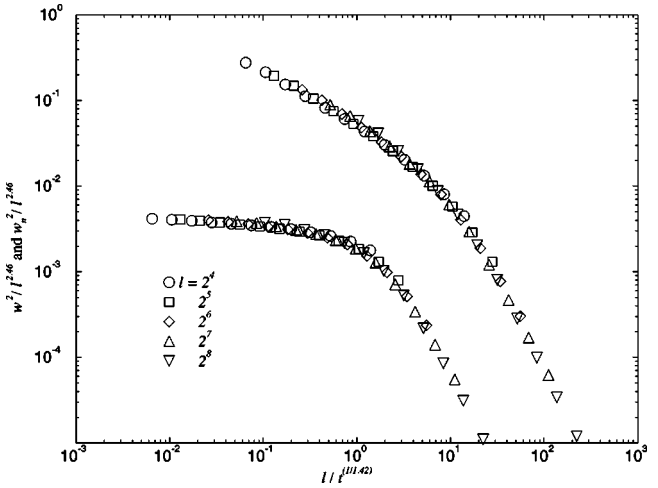

FIG. 3. The data collapse of $w^2(l,t)/l^{2\chi}$ (on the right) and $w_n^2(l,t)/l^{2\chi}$ (on the left) vs $l/t^{1/z}$ for $l=16, 32, \ldots, 256$, at $p=p_c$, with $2\chi=2.46$ and $z=1.42$. The data for $w^2(l,t)/l^{2\chi}$ have been shifted to the right by one decade for visibility.

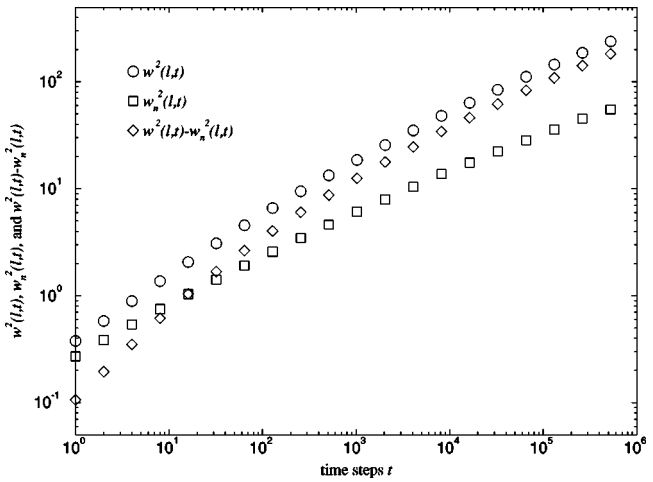

FIG. 4. The log-log plot of $w^2(l,t)$ (circle), $w_n^2(l,t)$ (square), and $w^2(l,t)-w_n^2(l,t)$ (diamond) vs time t, for $l=8$, of the DT model.

slopes. In order to know whether $w_n(l,t)$ retrieves ordinary dynamic scaling behaviors, we perform data collapse for $w_n(l,t)$ with a set of different l's and t's. In Fig. 3, we obtain excellent data collapse for both $w^2(l,t)/l^{2\chi}$ (the right data collapse) and $w_n^2(l,t)/l^{2\chi}$ (the left data collapse) vs $l/t^{1/z}$, with $l=16,32,\ldots,256$ and $t\geqslant 32$ time steps, at $p=p_c$, by inserting the values of the roughness exponent ($\chi=1.23$) and the dynamic exponent ($z=1.42$). Thus $w_n(l,t)$ retrieves ordinary dynamic scaling behaviors. This distinct behavior can be understood as follows. The growth rules of the Leschhorn model allow the formation of large slopes in the interface, but restrict the magnitude of slope variation in the spatial direction. Thus, within a local window of size l ($\ll$ the system size L), the interface looks like a typical kinetically roughened interface tilted in a new direction. This crucial feature explains why the Leschhorn model exhibits both super-roughness and single scaling at the same time; moreover, the local interface roughness relative to the local orientation retrieves the ordinary dynamic scaling behavior. This argument can also be used to explain the behaviors of the curvature model [3], which is widely accepted as a prototype for describing many physical processes.

Next, we study the DT model. Fig. 1(b) is the interfacial configuration $h(x,t)$ vs the lattice site x, with the system size $L=512$ and time $t=65536$ ML, for the DT model. Figure 1(b) shows the formation of extremely narrow and deep grooves in the interface, which is the signature pattern for the super-rough growth models with spatial multiscaling behaviors [4]. Figure 4 is a log-log plot of $w^2(l,t)$ (circle), $w_n^2(l,t)$ (square), and $w^2(l,t)-w_n^2(l,t)$ (diamond) vs time t, for a local window size $l=8$, of the DT model. The number of realizations is equal to 100, and the system size $L=16384$. We see that $[w^2(l,t)-w_n^2(l,t)]^{1/2}$, proportional to the magnitude of the slope of the local interfacial configuration, cannot represent the whole anomalous time-dependence effect of the original local width $w(l,t)$ in the regime $l\ll t^{1/z}\ll L$ with the dynamic exponent $z=3.74$ [4]. Figure 4 clearly shows that $w_n(l,t)$, the local interfacial roughness relative to the local orientation in a window of size l, still increases with time even when $t\gg l^z$. In addition, both $[w^2(l,t)-w_n^2(l,t)]^{1/2}$ and $w_n(l,t)$ have the same anomalous temporal scaling as the original local width $w(l,t)$. This *robust anomalous dynamic scaling* behavior is a unique feature of super-rough growth models which exhibit spatial multiscaling. It occurs because the growth rules of these models allow not only the formation of large slopes but also a large variation of the slopes in the spatial direction. The interface gradually forms very steep and narrow local grooves as time increases. Thus, within the local window (of the fixed size), the interface roughness relative to the local orientation still increases with time even in the late time regime. This behavior is in sharp contrast to that of super-rough models with single scaling.

For growth models which obey the ordinary dynamic scaling ansatz, the new definition of the local width $w_n(l,t)$ still displays the same scaling behaviors as the original one $w(l,t)$. Here we choose the Family model as an example. The roughness exponent χ and the dynamic exponent z for the Family model are 0.50 and 2.0, respectively [4]. Thus $w^2(l,t)$ in the long time limit, i.e., $t\gg l^z$ ($=l^2$), saturates and

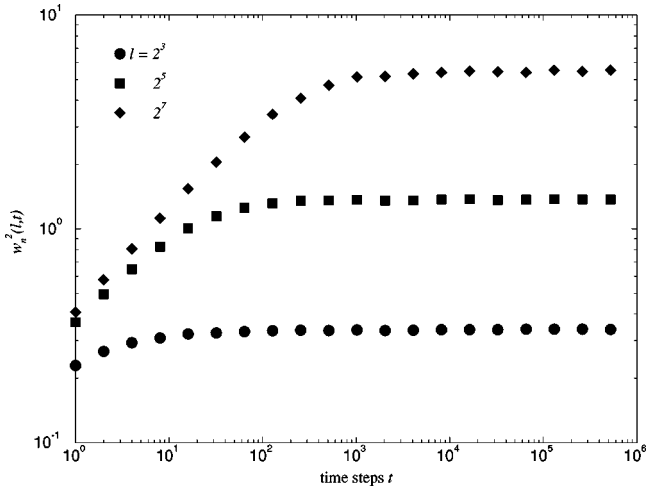

FIG. 5. The log-log plot of $w_n^2(l,t)$ vs time t, for $l=8$, 32, and 128 (from bottom to top), of the Family model.

scales as $l^{2\chi}$ $(=l)$. Figure 5 is the log-log plot of $w_n^2(l,t)$ vs time t, for $l=8$, 32, and 128 (from bottom to top) of the Family model. The number of realizations is equal to 100, and the system size $L=4096$. This clearly shows that $w_n^2(l,t)$ saturates in the long time limit, i.e., $t \gg l^2$. In addition, the saturated values for $w_n^2(l,t)$ $(=0.34, 1.37,$ and 5.46 for $l=8$, 32, and 128, respectively) scale as l. Thus $w_n(l,t)$ indeed demonstrates the same scaling behaviors as $w(l,t)$.

In conclusion, we propose a new definition of the local interfacial width $w_n(l,t)$, which is the roughness of the interface relative to the average interfacial orientation in a local window of size l. Then two major classes of super-rough growth models, one displaying single scaling behaviors and the other spatial multiscaling behaviors, are numerically studied in detail. We find that the interface belonging to the former class consists of global grooves with a horizontal size comparable to the system size L; thus the local interfacial width retrieves the ordinary dynamic scaling behavior under the new definition. In contrast, we find that the interface belonging to the latter class consists of many local grooves with deep valleys and narrow horizontal sizes; thus the local interfacial width still retains anomalous dynamic scaling behaviors under the new definition. This *robust anomalous dynamic scaling behavior* is a unique feature of super-rough models with spatial multiscaling. In addition, for growth models obeying the ordinary dynamic scaling ansatz, $w_n(l,t)$ still displays the same scaling behaviors as the original local width. We see that the measurement of $w_n(l,t)$ not only gives values of the scaling exponents like those found from the measurement of $w(l,t)$, but also discerns the robust anomalous dynamic scaling behavior among systems which exhibit super-roughness. Thus it gives us very important information for pinning down possible models to describe the experimental growth processes.

Note added. Recently we were informed that a technique similar to the subtraction in $w_n(l,t)$ has been employed in the analysis of weather data [18].

The work of N.-N.P. was supported in part by the National Science Council of the Republic of China under Grant No. NSC 89-2112-M-002-012.

[1] See, for example, A.-L. Barabási and H. E. Stanley, *Fractal Concepts in Surface Growth* (Cambridge University Press, Cambridge, 1995); T. Halpin-Healy and Y.-C. Zhang, Phys. Rep. **254**, 215 (1995); J. Krug, Adv. Phys. **46**, 139 (1997).
[2] F. Family and T. Vicsek, J. Phys. A **18**, L75 (1985).
[3] J. Krug, Phys. Rev. Lett. **72**, 2907 (1994).
[4] S. Das Sarma, C. J. Lanczycki, R. Kotlyar, and S. V. Ghaisas, Phys. Rev. E **53**, 359 (1996).
[5] J. M. López and M. A. Rodríguez, J. Phys. I **7**, 1191 (1997).
[6] N.-N. Pang and W.-J. Tzeng, Phys. Rev. E **59**, 234 (1999).
[7] A. Brú *et al.*, Phys. Rev. Lett. **81**, 4008 (1998).
[8] S. Morel, J. Schmittbuhl, J. M. López, and G. Valentin, Phys. Rev. E **58**, 6999 (1998).
[9] H.-N. Yang, Y.-P. Zhao, G.-C. Wang, and T.-M. Lu, Phys. Rev. Lett. **76**, 3774 (1996).
[10] J. H. Jeffries, J. K. Zuo, and M. M. Craig, Phys. Rev. Lett. **76**, 4931 (1996).
[11] H. Leschhorn, Physica A **195**, 324 (1993).
[12] S. Das Sarma and P. Tamborenea, Phys. Rev. Lett. **66**, 325 (1991).
[13] R. Bruinsma and G. Aeppli, Phys. Rev. Lett. **52**, 1547 (1984).
[14] J. Koplik and H. Levine, Phys. Rev. B **32**, 280 (1985).
[15] F. Family, J. Phys. A **19**, L441 (1986).
[16] S. F. Edwards and D. R. Wilkinson, Proc. R. Soc. London, Ser. A **381**, 17 (1982).
[17] J. G. Amar, P.-M. Lam, and F. Family, Phys. Rev. E **47**, 3242 (1993).
[18] E. Koscielny-Bunde *et al.*, Phys. Rev. Lett. **81**, 729 (1998).